ELSEVIER

Journal of Alloys and Compounds 275–277 (1998) 746–749

Journal of ALLOYS AND COMPOUNDS

Luminescence properties of rare earth ions in polytantalate

Shun-ichi Kubota[a,*], Hiasanori Yamane[a], Masahiko Shimada[a], Hirotsugu Takizawa[b], Tadashi Endo[b]

[a]*Institute for Advanced Materials Processing, Tohoku University, Katahira, Aoba-ku, Sendai, Miyagi 980-77, Japan*

[b]*Department of Molecular Chemistry and Engineering, Faculty of Engineering, Tohoku University, Aoba, Aoba-ku, Sendai, Miyagi 980-77, Japan*

Abstract

The luminescence properties of R^{3+} ($R^{3+}=Eu^{3+}$, Tb^{3+}, Tm^{3+}) in $La_{1-x}R_xTa_7O_{19}$ solid solution were systematically examined. In this host lattice, the distance between nearest neighbors of the La^{3+} site which were substituted by the R^{3+} ions, were very long (about 0.62 nm) and the sites locate two-dimensionally. The critical concentration at which the concentration quenching occurred under UV excitation were $x=1.0$ in $La_{1-x}Eu_xTa_7O_{19}$, $x=0.9$ in $La_{1-x}Tb_xTa_7O_{19}$ and $x=0.14$ in $La_{1-x}Tm_xTa_7O_{19}$. Furthermore the energy migration process of these samples were investigated. © 1998 Elsevier Science S.A.

Keywords: Luminescence; Rare earth; Energy migration; Tantalate

1. Introduction

A commonly encountered phenomenon in lattices which contain luminescent ions is the quenching of the luminescence when the concentration of these ions is increased. This may be due to cross-relaxation, or to energy migration to quenching centers where the excitation energy is lost nonradiatively. These quenching sites, or killers, may be impurities or defects, which inevitably present in the lattice.

In the course of our investigation on emission character of the phosphor in which the concentration quenching hardly takes place, concentrated rare earth systems, we reported recently on the luminescence properties of $LaTa_7O_{19}$:Eu^{3+} [1], $LaTa_7O_{19}$:Tb^{3+} [2] and $LaTa_7O_{19}$:Tm^{3+} [3]. The critical concentrations at which the concentration quenching occurred under UV excitation were $x=0.9$ in $La_{1-x}Tb_xTa_7O_{19}$, $x=0.14$ in $La_{1-x}Tm_xTa_7O_{19}$ and $x=1.0$ in $La_{1-x}Eu_xTa_7O_{19}$, i.e. no concentration quenching occurred.

In general, the energy transfer between activator ions that causes concentration quenching are caused by multipole–multipole interactions and exchange interactions [4,5]. Because of the reciprocal dependence on the distance between activator ions, a, in the case of multipole–multipole interactions (a^{-6}; a^{-8}; a^{-10} ...) and the exponential dependence on a ($\exp(-a/L)$) in the case of exchange interaction, the interaction strengths between activator ions decrease with increasing a.

RTa_7O_{19} (R=rare earths, except Yb^{3+} and Lu^{3+}) were known to be isostructural of $CeTa_7O_{19}$ [6]. In this crystal structure, the networks of $(R,Ta)O_8$ were interstratified in the double layer of TaO_7^{9-}. The distance between these layers, 1 nm, is considerably larger than the nearest-neighbor distance between two R^{3+} ions in the networks, 0.62 nm. This value is larger than that of other phosphors. So it was expected for RTa_7O_{19} that the critical concentration of concentration quenching was higher than other phosphors. Recently we reported the energy migration processes in $EuTa_7O_{19}$, $TbTa_7O_{19}$ and $La_{0.86}Tm_{0.14}Ta_7O_{19}$ [7]. The decay characteristics of the Eu^{3+} and Tb^{3+} emission can be explained by using a quasi-two-dimensional migration model, not by a two-dimensional migration model. On the other hand, the characteristics of the Tm^{3+} emission can be explained by using the cross-relaxation energy transfer model.

2. Experimental

2.1. Preparation

La_2O_3 and rare earth oxides (Rare Metallic Co. Ltd., purity of >99.99% purity) were intimately mixed in the desired properties, and dissolved in the hot 6N–HNO_3 solution. Successively, Ta_2O_5 (Rare Metallic Co. Ltd., purity of >99.99%) was added into the nitrate solutions. After evaporation to dryness, the products were calcined at 800°C for 6 h in air. The recovered powder was pressed at

*Corresponding author.

0925-8388/98/$19.00
PII: S0925-8388(98)00426-5

100 MPa to form a disc, and then calcined in air at 1200°C for 24 h. Occasionally, the procedure was followed by regrinding, repelleting and refiring two times to make its composition uniform.

2.2. Characterization

The identification of samples were performed identified by a Shimazu XR-610 diffractometer system with Ni-filtered Cu Kα radiation. The emission and excitation spectra were obtained by a Shimazu RF-540 spectrophotometer equipped with Xenon lamp.

3. Results and discussion

Fig. 1 shows the emission spectra of $EuTa_7O_{19}$, $La_{0.1}Tb_{0.9}Ta_7O_{19}$ and $La_{0.86}Tm_{0.14}Ta_7O_{19}$ under UV excitation, measured at room temperature. The emission spectrum of Eu^{3+} in $EuTa_7O_{19}$ consists of a strong peak at 610 nm and several weak peaks. These peaks correspond to transitions $^5D_j \rightarrow {}^7F_{j'}$ (j=0, 1; j'=0, 1, 2, 3, 4) [8]. Similar spectra were observed in the solid solution for all concentrations with the change of intensity. The ratio of the $^5D_0 \rightarrow {}^7F_1$ (magnetic-dipole transition) and $^5D_0 \rightarrow {}^7F_2$ (electric-dipole transition) indicates that Eu^{3+} sites had no inversion symmetry. For $La_{0.1}Tb_{0.9}Ta_7O_{19}$, the peaks are assigned to the transitions $^5D_4 \rightarrow {}^7F_j$ (j=3, 4, 5, 6) of Tb^{3+} [9]. The intensity of emission from $^5D_3$ decreases gradually with increasing the Tb^{3+} concentration in $La_{1-x}Tb_xTa_7O_{19}$. The observation shows that cross-relaxation obviously takes place in the transitions $^5D_3 \rightarrow {}^5D_4 \Rightarrow {}^7F_6 \rightarrow {}^7F_0$ and/or $^5D_3 \rightarrow {}^7F_0 \Rightarrow {}^7F_6 \rightarrow {}^5D_4$ [10–12]. For $La_{0.86}Tm_{0.14}Ta_7O_{19}$, the peaks are assigned to the transitions $^1D_2 \rightarrow {}^3H_4$ [13].

In order to study the concentration dependence of the luminescence in $La_{1-x}R_xTa_7O_{19}$ (R^{3+}=Eu^{3+}, Tb^{3+}, Tm^{3+}; $0<x\leq 1$), the emissions under UV excitation were measured as a function of the concentration x at room temperature. Fig. 2 shows the results. The intensity increases with increasing the concentration up to x=1.0 for $La_{1-x}Eu_xTa_7O_{19}$. Those results indicated that $La_{1-x}Eu_xTa_7O_{19}$ had a very high critical concentration. In $EuTa_7O_{19}$, the EuO_8^{13-} octahedra, which were formed by the Eu^{3+} ion and its surrounding O^{2-} ions, were isolated

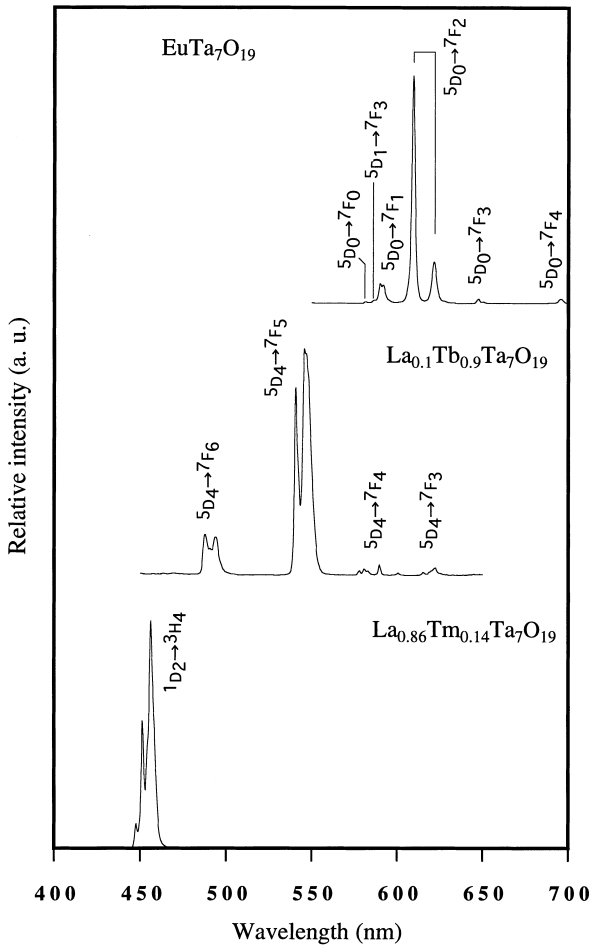

Fig. 1. Emission spectra of the Eu^{3+} in $EuTa_7O_{19}$ (exc. 396.3 nm), Tb^{3+} in $La_{0.1}Tb_{0.9}Ta_7O_{19}$ (exc. 380.4 nm) and Tm^{3+} in $La_{0.86}Tm_{0.14}Ta_7O_{19}$ (exc. 359 nm).

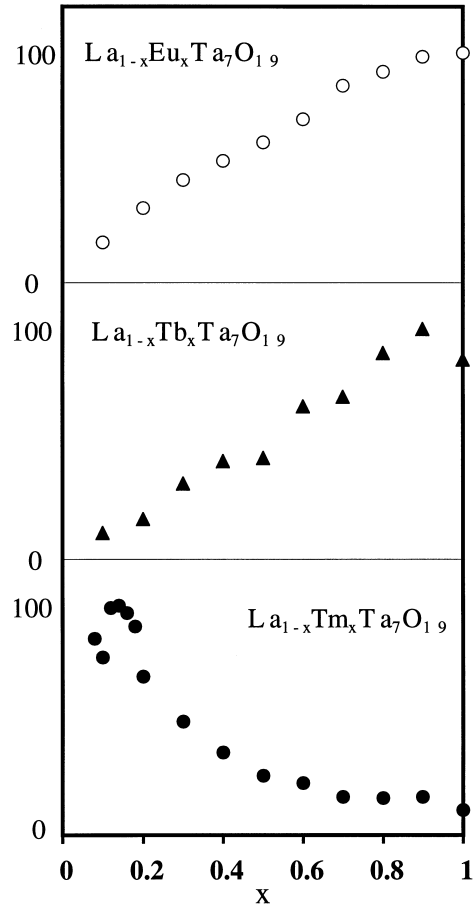

Fig. 2. Concentration x dependences of the emission intensity in $La_{1-x}Tm_xTa_7O_{19}$ (em. 456 nm) ($0<x\leq 1$).

from each other by TaO_7^{9-} and TaO_8^{11-} polyhedra. There were no ions common to any Eu^{3+} ions [6]. It seemed that interaction between the Eu^{3+} ions was caused by dipole interaction [14]. The probabilities of those interactions were decreasing with increase in the separation between Eu^{3+} ions [4,5]. The energy migration to killer sites resulting in concentration quenching was restricted by the long separation and, described in Ref. [15], the low dimensionality of the sites. This indicated that the interaction between Eu^{3+} ions was very weak in $La_{1-x}Eu_xTa_7O_{19}$. For $La_{1-x}Tb_xTa_7O_{19}$, the intensity of the emission proportionally increases with increasing concentration up to $x=0.9$. It seemed that the energy migration to killer sites resulting in concentration quenching was restricted by the long separation and the low dimensionality of the sites, as was the case in $La_{1-x}Eu_xTa_7O_{19}$. On the other hand the critical concentration was very low, $x=0.14$, in $La_{1-x}Tm_xTa_7O_{19}$.

In order to investigate on the energy migration processes, we analyzed the decay curves measured at room temperature [7]. Fig. 3 shows a semilogarithmic decay curve of the Eu^{3+} emission in $EuTa_7O_{19}$. As mentioned above, in $EuTa_7O_{19}$, the distance between Eu^{3+} layers (~1.0 nm) is slightly larger than the nearest-neighbor distance between two Eu^{3+} ions in the layer (~0.62 nm). This implies that migration among Eu^{3+} ions occurs in the layer. For this reason we tried to fit the decay curves for two-dimensional migration [16]. In spite of the structural anisotropy of $EuTa_7O_{19}$, the decay characteristics could not be described by a two-dimensional diffusion model. This fact indicates that no complete two-dimensional energy migration occurs in $EuTa_7O_{19}$. Berdowski et al. explained the energy migration in EuOCl by using a quasi-two-dimensional energy migration, i.e. a two-dimensional energy migration which partially concludes three-dimensional energy migration [17]. They tried to fit the measured decay curve to Eq. (1), the Yokota–Tanimoto expression. This expresses a three-dimensional diffusion-limited energy migration [18].

$$I(t) = I(0)\exp(-P_r t)\exp\left[-\frac{4}{3}\pi^{3/2}N_a(Ct)^{1/2}\left(\frac{1+10.87x+15.50x^2}{1+8.743x}\right)^{3/4}\right]$$
$$x = DC^{1/3}t^{2/3} \quad (1)$$

where C is the coupling constant for donor–acceptor interaction, D the diffusion constant and N_a the acceptor concentration.

Then they calculated the diffusion constant with the help of Eq. (2) which expresses the effective diffusion constant of quasi-two-dimensional diffusion.

$$D = (D_2 - D_1)^{1/2}D_2^{1/2}/\tanh^{-1}\left(1-\frac{D_1}{D_2}\right)^{1/2} \quad (2)$$

where D_2 is the diffusion constant in the layers and D_1 is the diffusion constant between layers. We tried to analyze the decay curves by the quasi-two-dimensional migration model. In order to estimate N_a, acceptor concentration of the sample, we have synthesized $Eu_{0.99}Nd_{0.01}Ta_7O_{19}$ and measured its emission decay. Table 1 presents experimental data on the Eu^{3+}–Eu^{3+} distance a, dimensionality of Eu^{3+} sublattice d, concentration for which emission intensity was maximum x_{max}, probability for transfer within the donor system P, and diffusion constant D of Eu^{3+} phosphors at room temperature. From Table 1 it is clear that the transfer probability in $EuTa_7O_{19}$ is less than other phosphors, except that EuP_3O_9 and that $EuTa_7O_{19}$ have high x_{max} values. This is explained by the fact that the resonance transfer is reduced by the long distance between Eu^{3+} ions and that the probability that the migration excitation encounters one of the randomly distributed traps, is reduced by a low dimensionality of Eu^{3+} sublattice. Furthermore the decay characteristics of the Tb^{3+} emission in $TbTa_7O_{19}$ can be explained by using a quasi-two-dimensional migration model, not by a two-dimensional migration model. On the other hand, the characteris-

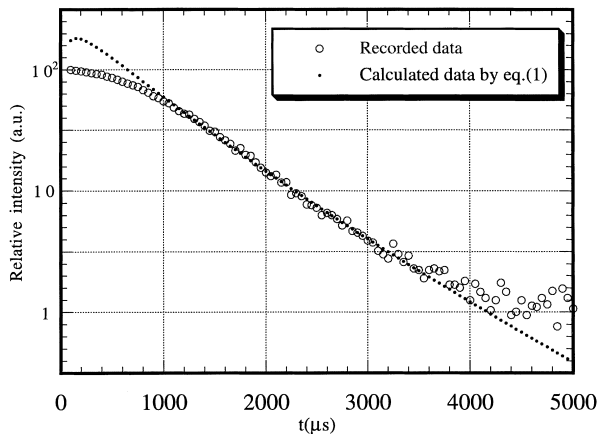

Fig. 3. Semilogarithmic decay curve of the Eu^{3+} emission in $EuTa_7O_{19}$ (exc. 535 nm; em. 610 nm), fitting curve to Eq. (1).

Table 1
Experimental data on Eu^{3+}–Eu^{3+} distance a, dimensionality of Eu^{3+} sublattice d, concentration for which emission intensity was maximum x_{max}, probability for transfer within the donor system P, and diffusion constant D of Eu^{3+} phosphors at room temperature

Compound	a (nm)	d	x_c	P (s^{-1})	D ($cm^2\ s^{-1}$)	Ref.
$NaEuTiO_4$	0.37	2	0.3	5.8×10^7	2×10^{-8}	[7]
$EuMgB_5O_{10}$	0.40	1	0.85	10^7	—	[19]
$Li_6Eu(BO_3)_3$	0.39	1	—	10^7	—	[20]
EuOCl	0.37	2	0.1	1.7×10^6	5.8×10^{-10}	[16]
$EuAl_3B_4O_{12}$	0.59	3	0.3	1.3×10^6	8×10^{-10}	[21]
EuP_3O_9	0.42	1	1.0	7×10^5	—	[14]
$EuTa_7O_{19}$	0.62	2	1.0	1.2×10^6	1.2×10^{-9}	This work

tics of the Tm^{3+} emission can be explained by using the cross-relaxation energy transfer model [22].

4. Conclusion

$La_{1-x}Eu_xTa_7O_{19}$ and $La_{1-x}Tb_xTa_7O_{19}$ had high critical concentrations under UV excitation, showing that the energy migration between Eu^{3+} and Tb^{3+} ions was restricted by the long distance between nearest neighbors. The energy migration in $EuTa_7O_{19}$ and $TbTa_7O_{19}$ is strongly affected by the crystal structure. This migration is described as a quasi-two-dimensional energy migration which partially includes three-dimensional energy migration. The transfer probabilities of activator ions are less than those of other phosphors and x_{max} values are high. This is sustained by the fact that the resonance transfer is reduced by the long distance between activator ions, and the probability that the migration excitation encounters one of the randomly distributed traps is reduced by a low dimensionality of activator sublattice.

On the other hand, the energy migration in $La_{0.86}Tm_{0.14}Ta_7O_{19}$ is described as a three-dimensional energy migration in which the excitation energy is decreased by the cross-relaxation mechanism. The lower x_{max} of $La_{1-x}Tm_xTa_7O_{19}$ is explained by the fact that the critical radius for the cross-relaxation energy transfer is very long.

Acknowledgements

The present authors wish to thank Mr. T. Hase, Dr. N. Kijima and Dr. N. Shimomura of the Mitsubishi Kasei Co. Ltd. for fruitful discussions. This work was supported in part by a Grant-in-aid for Scientific Research (B) of the Ministry of Education, Science and Culture, Japan and IKETANI Science and Technology Foundation (No. 052025), Japan.

References

[1] S. Kubota, T. Endo, H. Takizawa, M. Shimada, J. Alloys Compounds 217 (1995) 44.
[2] S. Kubota, T. Endo, H. Takizawa, M. Shimada, J. Electrochem. Soc. 142 (1995) 4269.
[3] S. Kubota, T. Endo, H. Takizawa, M. Shimada, J. Alloys Compounds 210 (1994) 103.
[4] T. Förster, Ann. Phys. 2 (1948) 55.
[5] D. Dexter, J. Chem. Phys. 21 (1953) 836.
[6] B.M. Gatehouse, J. Solid State Chem. 27 (1979) 209.
[7] S. Kubota, M. Shimada, H. Takizawa, T. Endo, J. Alloys Compounds 241 (1996) 16.
[8] G.H. Dieke, in: H.M. Crosswhite, H. Crosswhite (Eds.), Spectra and Energy levels of Rare Earth Ions in Crystals, Interscience, New York, 1968, p. 242.
[9] G.H. Dieke, in: H.M. Crosswhite, H. Crosswhite (Eds.), Spectra and Energy levels of Rare Earth Ions in Crystals, Interscience, New York, 1968, p. 253.
[10] G. Blasse, A. Bril, Philips Res. Rep. 22 (1967) 481.
[11] G. Blasse, J. Luminesc. 1(2) (1970) 766.
[12] D.J. Robbins, B. Cockayne, B. Lent, J.L. Glasper, Solid State Commun. 20 (1976) 673.
[13] G.H. Dieke, in: H.M. Crosswhite, H. Crosswhite (Eds.), Spectra and Energy levels of Rare Earth Ions in Crystals, Interscience, New York, 1968, p. 309.
[14] M. Buijs, G. Blasse, J. Luminesc. 39 (1988) 323.
[15] H. Yamamoto, Oyobuturi (in Japanese) 42 (1973) 1246.
[16] P.A.M. Berdowski, G. Blasse, J. Luminesc. 29 (1984) 243.
[17] P.A.M. Berdowski, J. Van Herk, G. Blasse, J. Luminesc. 34 (1985) 9.
[18] M. Yokota, O. Tanimoto, J. Phys. Soc. Jpn. 22 (1967) 779.
[19] M. Buijs, G. Blasse, J. Luminesc. 34 (1986) 263.
[20] Fu Wen Tian, C. Fouassier, P. Hagenmuller, J. Phys. Chem. Solids 48 (1987) 245.
[21] F. Kellendonk, G. Blasse, J. Chem. Phys. 75 (1981) 561.
[22] C. Li, A. Lagriffoul, R. Moncorge, J.C. Souriau, C. Borel, Ch. Wyon, J. Luminesc. 62 (1994) 157.